Cytometry 20:281–289 (1995)

Changes in Intracellular Calcium Concentration and pH of Target Cells During the Cytotoxic Process: A Quantitative Study at the Single Cell Level

Katarina Radošević, Bart G. de Grooth, and Jan Greve[1]

Department of Applied Physics, Applied Optics Group, University of Twente, Enschede, The Netherlands

Received for publication September 29, 1994; accepted February 17, 1995

This study reports on the changes in intracellular calcium concentration ($[Ca^{2+}]_{in}$) and intracellular pH ($[pH]_{in}$) that occur in K562 target cells during interaction with human Natural Killer (NK) cells. The data were obtained using a quantitative fluorescence microscope and fluorescent ratio probes specific for $[Ca^{2+}]_{in}$ (Fura-2-AM) and $[pH]_{in}$ (BCECF-AM). Results demonstrate that two types of target cell response to the attack by an NK cell can be distinguished. The target cell either dies immediately, due to the complete breakdown of the membrane impermeability, or the initial membrane damage (i.e., increased membrane permeability) is repaired and the cell "escapes" immediate death. During both responses an increase of $[Ca^{2+}]_{in}$ takes place in the target cells. In the cells that die immediately, however, $[Ca^{2+}]_{in}$ reaches higher levels (approximately 1,400 nM) than in the cells that restore the initial damage (approximately 700 nM). Changes in target cell $[pH]_{in}$ are also detected during both responses. The direction of the change (acidification or alkalinization) as well as the level of the change depend on extracellular pH ($[pH]_{ex}$). Also, $[pH]_{in}$ remains changed during the time the cells were followed (10 min). The programming time (i.e., the time from the initiation of the cytotoxic process to the time that a change in the physiological parameter was detected) of the killing process that leads to an immediate target cell death appears to be shortest at $[pH]_{ex}$ 7.3–7.6 (approximately 3 min). © 1995 Wiley-Liss, Inc.

Key terms: Natural Killer cell, cytotoxic activity, target cell, calcium, pH, fluorescent ratio probes

The interaction between cytotoxic cells and target cells has been the subject of numerous studies (4,7, 12,22,27,30). The exact killing mechanism, however, has not been resolved yet.

It is generally accepted that perforin (pore forming protein) plays an important role during the cytotoxic process (7,27,30). However, the existence of additional killing mechanism(s) is suggested by the fact that killing can occur in the absence of calcium, a condition necessary for the action of perforin, and also in the absence of detectable degranulation (18,29). Moreover, perforin-deficient killer cells can still be cytotoxic to certain types of target cells, albeit with a lower efficiency (10).

The evidence that the interaction with a killer cell can lead to DNA fragmentation in the target cell raises again the question of the cause of target cell death (4,12,22). The enzymes directly responsible for the DNA damage have not yet been identified. It was reported that both perforin and granzyme A are needed in order to obtain significant DNA fragmentation (15). This indicates that perforin not only can kill by damaging the cell membrane, but may also act as a helper molecule for other target cell damaging molecules. One possibility is that the channels formed by perforin molecules in the cell membrane ensure the "entrance" of other toxic agents into the target cell. Thus, different killing mechanisms need not be mutually exclusive (31). Besides granzyme A, some other enzymes have also been proposed to play a key role in damaging the DNA (16,24,25).

The cellular physiology is greatly affected by the processes that lead to cell damage (5). A change in the intracellular calcium homeostasis appears to be not only a hallmark of cell activation but also generally accompanies cell death (17). It has been observed that the intracellular calcium concentration ($[Ca^{2+}]_{in}$) increases in the cells that are attacked by the cytotoxic cells (1,19, 28). In some cases this increase appeared to be a prerequisite for efficient cell killing (13,26). Although calcium can play a protective role, it may also, at high enough concentrations, trigger a destruction pathway in the cell (3).

Closely associated with the calcium homeostasis are

Address reprint requests to Jan Greve, Department of Applied Physics, Applied Optics Group, University of Twente, P.O. Box 217, 7500 AE Enschede, The Netherlands.

the membrane potential and the intracellular pH ($[pH]_{in}$), functioning in concert to maintain cellular integrity. Changes in the membrane potential of target cells, associated with the killing process, have been reported previously (21). A clear picture of the eventual changes in $[pH]_{in}$ has yet to be formed (28).

In order to get a better insight into the processes associated with target cell death, we have made an attempt to characterize the changes that occur in target cell $[Ca^{2+}]_{in}$ and $[pH]_{in}$ during a Natural Killer (NK) cell attack. We have done so by performing quantitative fluorescence microscopy of the target cells labeled with ratio probes specific for $[Ca^{2+}]_{in}$ (Fura-2-AM) and $[pH]_{in}$ (BCECF-AM).

MATERIALS AND METHODS

Chemicals

RPMI-1640 was obtained from Seramed (Berlin, Germany), fetal calf serum from Gibco (Gaithersburg, MD), and rIL-2 from PromoCell (Heidelberg, Germany). The antibiotics, L-glutamine, leucoagglutinin, nigericin, EGTA, and poly-L-lysine hydrobromide (PLL; mol wt 70–150 kDa) were purchased from Sigma Chemical Co. (St. Louis, MO). Hepes and Na_2 EDTA were obtained from Merck (Darmstadt, Germany). Pluronic F-127, 4-Br A-23187, and fluorescent probes (Fura-2-AM, BCECF-AM, and BCECF-acid) were purchased from Molecular Probes (Eugene, OR).

Cells

NK cells, clone NK76, phenotype CD2+3−16+56+, were cultured in 96-well plates in RPMI-1640 medium, supplemented with 25 mM Hepes, 2 mM L-glutamine, 10% pooled human serum, 100 U/ml penicillin, 100 μg/ml streptomycin, 1 μg/ml indomethacin, 1 μg/ml leucoagglutinin (PHA-L), and 25 U/ml rIL-2. Cells were subcultured each 7th day on a layer of 30 Gy irradiated feeder cells that consisted of the mixture of APD and BSM cells (Epstein-Barr virus-transformed B-cell lines), and peripheral blood lymphocytes.

K562 cells (human cell line derived from a patient with myelogenous leukemia) were maintained in exponential growth phase in RPMI-1640 medium, supplemented with 10% fetal calf serum, 2 mM L-glutamine, 100 U/ml penicillin, and 100 μg/ml streptomycin.

Labeling Procedures

Labeling with Fura-2-AM. A stock solution of Fura-2-AM was prepared in dimethylsulfoxide (DMSO; 1 mM). The working solution was prepared by mixing 9 parts of Fura-2-AM stock solution with 1 part of 20% Pluronic F-127 in DMSO (dissolved by heating to 40°C). Cells were resuspended in RPMI-1640/Hepes at a concentration of 10^6 cells/ml. Fura-2-AM working solution was added to the cell suspension (final concentration 5 μM) and the suspension was incubated in the dark at room temperature for 30 min. The cells were washed twice with RPMI-1640/Hepes and resuspended in RPMI-1640/Hepes supplemented with 10% fetal calf serum, L-glutamine, and antibiotics, pH 7.3 (further referred to as complete medium).

Labeling wth BCECF-AM. A stock solution of BCECF-AM was prepared in DMSO (5 mM). K562 cells were resuspended in RPMI-1640/Hepes at a concentration of 10^6 cells/ml. BCECF-AM stock solution was added to the cell suspension (final concentration 5 μM) and the suspension was incubated in the dark at 37°C for 30 min. The cells were washed twice with RPMI-1640/Hepes and resuspended in complete medium. All labeled cells were kept at 4°C until used.

Conjugate Formation and Experimental Approach

NK cells and K562 cells were separately resuspended in complete medium containing 2 mM EDTA, at a concentration of 2×10^6 cells/ml. Fifty microliters of both cell suspensions was mixed and centrifuged for 5 min at 200*g*. The cell mixture was then gently resuspended and the cells were plated on a coverglass that was first coated with PLL (0.01% PLL/phosphate buffered saline [PBS], overnight) and then mounted in a holder (which enables keeping the cells in the incubation medium). The cells were allowed to attach for 15 min at room temperature. The holder was mounted on the microscopic stage. The cytotoxic process was initiated by changing the EDTA medium for complete medium (with one washing step) without moving the holder from the stage. All experiments were performed at approximately 25°C.

As determined using flow cytometric cytotoxicity assay (20), no killing was taking place in the presence of EDTA.

Ratio Measurements

The ratio measurements were performed using an inverted fluorescence microscope (IMT-2, Olympus Optical, Tokyo, Japan), equipped with an intensified CCD camera (C2400–87), a processor (DVS 3000), and a filter wheel (Berger Lahr), purchased from Hamamatsu Photonics (Herrsching am Ammersee, Germany).

For the measurements of calcium, a filter block consisting of a 350 ± 50 nm band pass filter (excitation), a 400 nm dichroic mirror, and a 420 nm long pass filter (emission) (Olympus Optical) was used. For the measurements of pH, a filter block consisting of a 450 ± 50 nm band pass filter (excitation), a 500 nm dichroic mirror, and a 515 nm long pass filter plus a 520 ± 20 nm band pass filter (emission) (Olympus Optical) was used.

The band pass filter pairs 340 ± 10/380 ± 10 nm and 490 ± 10/440 ± 10 nm (Omega Optical, Brattleboro, VT) were placed in the filter wheel and used to select the excitation wavelengths for the calcium and pH probes, respectively.

A 100 W Hg lamp was used as an excitation light source. The excitation intensity was attenuated using neutral gray filters. Fluorescence ratios were usually in the range of 0.8–3.1 for calcium (fluorescence intensity > 420 nm, excited at 340 nm/fluorescence intensity > 420 nm, excited at 380 nm) and ≤1 for pH (fluorescence intensity at 520 nm, excited at 490 nm/fluorescence intensity at

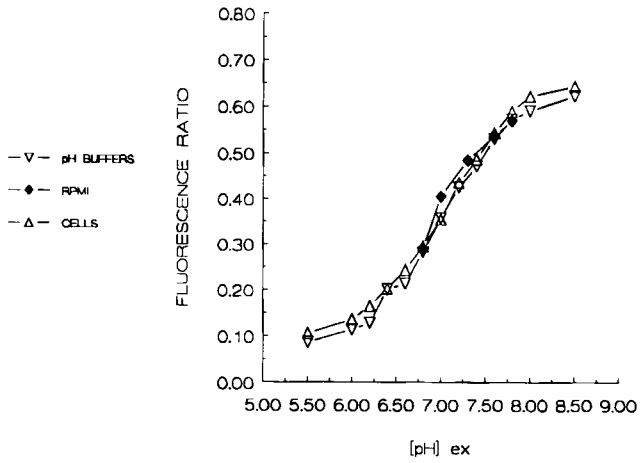

Fig. 1. pH calibration curves. The average fluorescence ratios of BCECF-acid in pH calibration buffers and complete medium of different pH were determined for in vitro calibration. The fluorescence ratios of 20 BCECF-AM-labeled K562 cells were determined in pH calibration buffers containing 5 μM nigericin (in situ calibration).

520 nm, excited at 440 nm). The fluorescence light was collected using a 100× oil-immersion objective, numerical aperture (N.A.) 1.30 (DPlanApo 100 UV, Olympus Optical).

The image acquisition and the data analysis were performed using the dedicated software package ICMS (Intracellular Ion Measuring System), purchased from Hamamatsu Photonics. All images were obtained by averaging 4 frames. The time interval between 2 ratio images was 120 ms. Image pairs were acquired every 30 s for the desired period of time. An average ratio was determined for each measured cell by defining cell borders on the brightfield images and then measuring the fluorescence within the border lines.

For pH measurement of the solutions, analyzing windows of approximate cell size were placed randomly over the image and the average ratio was determined.

Calibration Procedures

Calcium calibration buffers (8) contained 160 mM NaCl, 4.5 mM KCl, 1 mM $MgCl_2$, 5 mM Hepes, and 11 mM glucose. High calcium buffer also contained 10 mM $CaCl_2$, while low calcium buffer contained 10 mM EGTA. The pH was adjusted to 7.3. Fura-2-AM-labeled K562 cells were incubated in low calcium buffer containing 5 μM A23187 (Ca^{2+} ionophore; stock solution 5 mM in EtOH) for 5 min before collecting images for estimation of the minimum ratio, R_{min}. Subsequently, the buffer was changed to high calcium buffer containing A23187 and after equilibration the images for the estimation of the maximum ratio, R_{max},

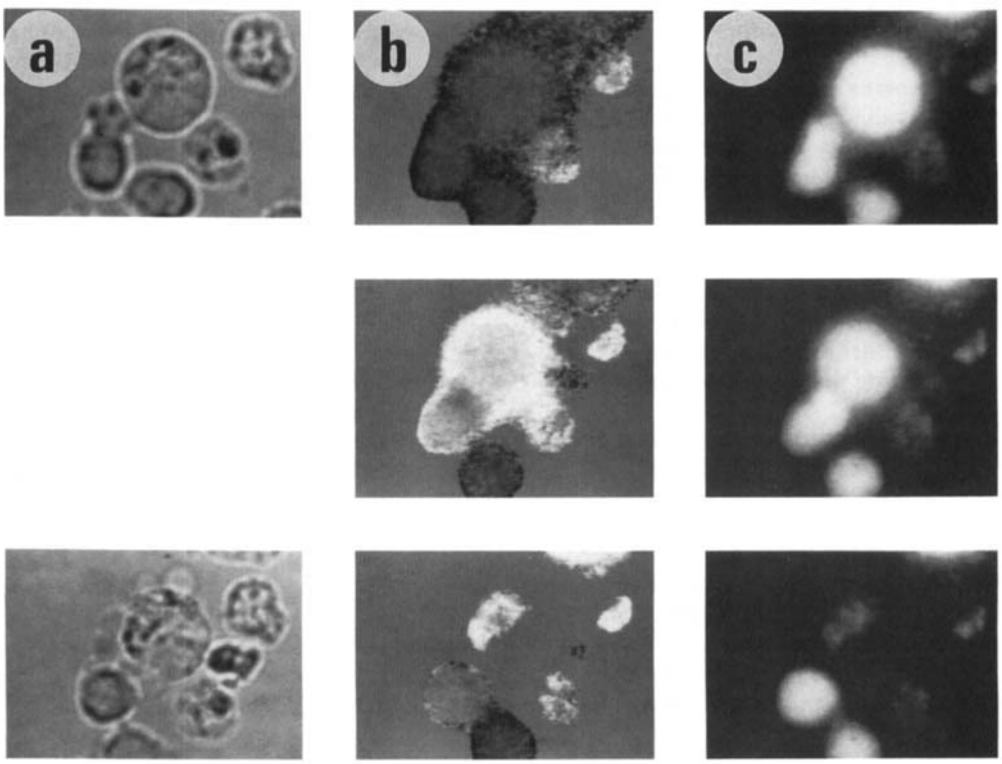

Fig. 2. Increase of $[Ca^{2+}]_{in}$ in the K562 cell during the NK cell attack. **a:** Brightfield image (middle cell K562 cell; bottom left cell NK cell). **b:** Ratio of Fura-2 (i.e., $[Ca^{2+}]_{in}$). **c:** Fluorescence upon 340 nm excitation of Fura-2. The brightness intensity corresponds to (b) ratio level and (c) fluorescence intensity. **Top:** Before the killing process (i.e., incubation in calcium-free medium); **middle:** 2 min incubation in calcium-rich medium; **bottom:** 6 min incubation in calcium-rich medium.

Table 1
$[pH]_{in}$ of K562 Cells in Complete Medium at Different pH[a]

$[pH]_{ex}$	6.80 ± 0.02	7.00 ± 0.02	7.30 ± 0.02	7.60 ± 0.02	7.80 ± 0.02
$[pH]_{in}$	6.93 ± 0.18	7.03 ± 0.13	7.13 ± 0.10	7.20 ± 0.10	7.25 ± 0.05

[a]The average $[pH]_{in}$ of BCECF-AM-labeled K562 cells incubated in complete medium of different $[pH]_{ex}$ was determined. At least 25 cells were measured for each $[pH]_{ex}$.

were collected. The calibration curve was calculated as follows (6):

$$[Ca^{2+}]_{in} = Kd \times [(R - R_{min})/(R_{max} - R)] \times (F_{low}/F_{high})$$

where Kd = dissociation constant of Fura-2 for Ca^{2+}; R, R_{min}, and R_{max} = actual, minimum, and maximum ratios, respectively; and F_{low} and F_{high} = fluorescence intensities upon 380 nm excitation in low and high calcium buffer, respectively.

The average R_{min} and R_{max}, determined in different calibration experiments, were 0.83 ± 0.04 and 3.14 ± 0.04, respectively. Assuming the Kd to be 225 nM in the cytosolic environment (6), the resting $[Ca^{2+}]_{in}$ in K562 cells was around 20 nM.

pH calibration buffers (2) contained 130 mM KCl, 1 mM $MgCl_2$, 15 mM 2-morpholinoethanesulphonic acid (MES), and 15 mM Hepes. The desired pH was adjusted with KOH. Complete medium was adjusted to the desired pH with NaOH and HCl.

In situ calibration curves were obtained using the pH calibration buffers containing 5 μM nigericin (K^+ ionophore, stock solution 10 mM in EtOH). BCECF-AM-labeled K562 cells were incubated with the first solution for 5–10 min to allow complete equilibration and then with subsequent solutions for 1 min before recording data.

In vitro standard solutions included 5 μM BCECF-acid (stock solution 5 mM in DMSO) in the pH calibration buffers and in complete medium, respectively. The solutions were measured using the coverglass holder with a mounted coverglass.

Figure 1 shows calibration curves obtained for pH buffers, complete medium at different extracellular pH, and K562 cells. As can be seen from Figure 1, similar curves were obtained for solutions and cells.

$[pH]_{in}$ of the control K562 cells was determined in complete medium at different extracellular pH, $[pH]_{ex}$. As can be seen from Table 1, $[pH]_{in}$ of K562 cells varied between 6.9 and 7.3, depending on $[pH]_{ex}$.

Calibration procedures were performed at 25°C, the same temperature as used in experiments during the cytotoxic process.

Statistical Analysis

The data are presented as mean ± S.D. Significance of differences was evaluated using the two-tailed t-test.

RESULTS

$[Ca^{2+}]_{in}$: Kinetics and Quantitation

Within a few minutes after the cytotoxic process was initiated an increase of $[Ca^{2+}]_{in}$ was detected in a fraction of the conjugated K562 target cells (Fig. 2B). Figure 3 shows that the increase was preceded by the movement of NK cell granules (arrows) toward the target cell, as demonstrated using fluorescence upon 380 nm excitation of Fura-2 (19). The increase was usually accompanied by a leakage of Fura-2 out of the cell, indicating an increase in the permeability of the target cell membrane (Fig. 2C). This is in agreement with the results of Poenie et al. (19). Complete loss of the dye was interpreted as a sign of cell death. In a fraction of the target cells, however, the observed increase of $[Ca^{2+}]_{in}$ was transient. In some of these cases an oscillating behavior was observed, while in others only a single increase was detected during an observation period of 10 min. The increase in membrane permeability of these cells was such that leakage of the dye was not complete. A few conjugates were followed up to 1 h and no additional change in $[Ca^{2+}]_{in}$ and membrane permeability could be detected.

In the following we refer to "dying cells" as those target cells that underwent complete loss of the dye (thus, complete breakdown of the membrane impermeability) within 10 min upon initial increase of $[Ca^{2+}]_{in}$. The target cells with a transient increase and no complete loss of Fura-2 within the same period are referred to as "transient cells." It should be noted that some of the cells we classified as transient may still have died later than 10 min after the initial increase took place.

Figure 4 shows the average changes in $[Ca^{2+}]_{in}$ as a function of time for dying (closed symbols) and transient (open symbols) target cells. Time 0 min indicates the last measurement before the change in the fluorescence ratio was detected. As can be seen from Figure 4, during the first 1.5 min $[Ca^{2+}]_{in}$ of both dying and transient cells increased drastically. $[Ca^{2+}]_{in}$ of transient cells increased on an average up to approximately 700 nM, followed by a decrease to a lower concentration (approximately 300 nM). In dying cells $[Ca^{2+}]_{in}$ increased up to approximately 1,400 nM as the cells approached death. Changes in $[Ca^{2+}]_{in}$ were observed neither in the non-conjugated K562 cells nor in the control K562 cells (incubated without NK cells).

$[pH]_{in}$ During the Cytotoxic Process

Since $[pH]_{in}$ represents another important physiological parameter, it is of interest to determine whether the

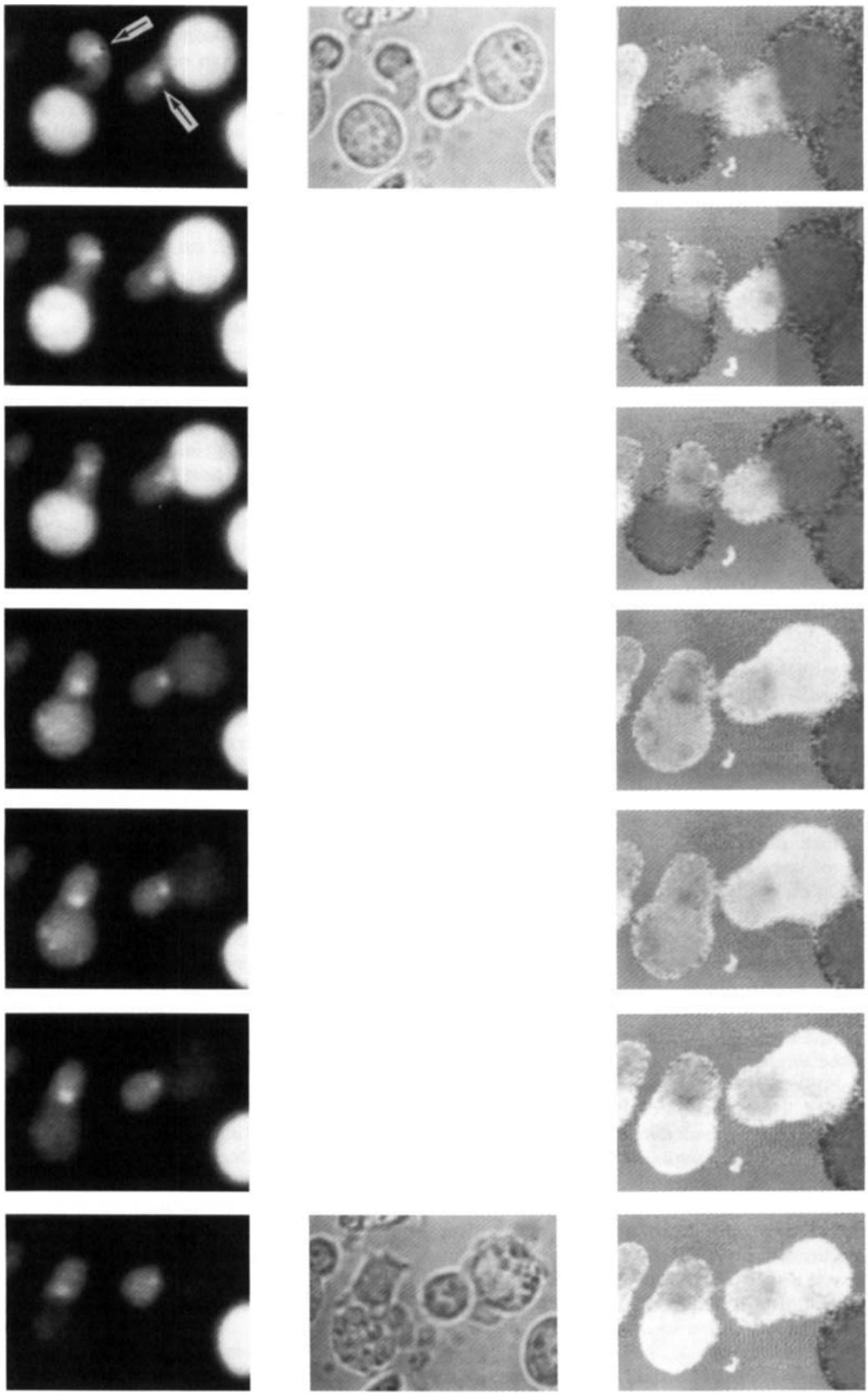

Fig. 3. View of the lethal hit. **Left:** Fluorescence upon 380 nm excitation of Fura-2. **Middle:** Bright field image. **Right:** Ratio of Fura-2 (i.e., $[Ca^{2+}]_{in}$). Images were taken upon 0, 1, 2, 3, 3.5, 4, and 5 min incubation in calcium-rich medium. The brightness intensity corresponds to fluorescence intensity (left) and ratio level (right). Notice the movements of the NK cell granules (arrows) toward the target cell.

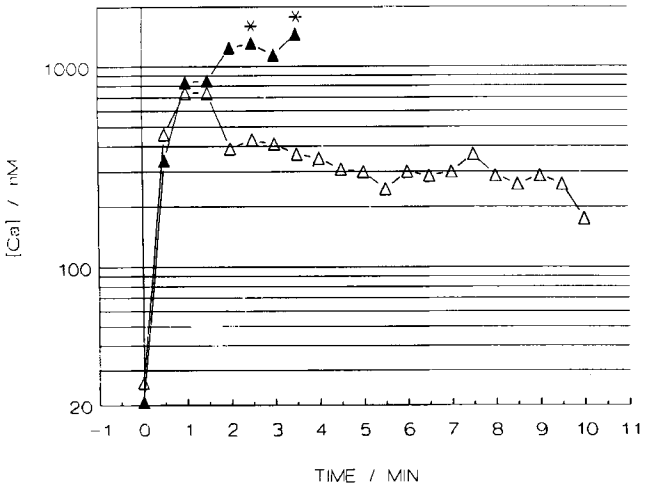

Fig. 4. Changes in $[Ca^{2+}]_{in}$ of dying (closed symbols) and transient (open symbols) K562 cells as a function of time. The average $[Ca^{2+}]_{in}$ of 15 transient cells is shown. For dying cells the number of cells available for averaging decreased gradually from 16 (first 2 points) to 4 (last 2 points) due to cell death (i.e., complete leakage of the dye out of the cells). Time 0 min indicates the last measurement before the increase of $[Ca^{2+}]_{in}$ was detected. *$P < 0.05$ (significantly different from the transient cells at the same time point).

attack by a killer cell causes changes in $[pH]_{in}$ of the target cell. Calcium measurements described above indicated, however, that the target cell membrane permeability increases upon interaction with a killer cell. This means that a change of $[pH]_{in}$, eventually observed during the killing process, may reflect the equilibration of $[pH]_{in}$ with $[pH]_{ex}$ and need not necessarily be the result of an active cellular process. In order to test this, we followed $[pH]_{in}$ of some target cells while interacting with killer cells in complete medium at different $[pH]_{ex}$ (6.8, 7.0, 7.3, 7.6, and 7.8). The membrane permeability of the target cells was monitored simultaneously, using the decrease in fluorescence emission of BCECF upon 440 nm excitation (relatively insensitive to pH). Both release and retention of BCECF were used previously for measurement of the cytotoxic activity (11).

Figure 5 (closed symbols) shows that during the cytotoxic process $[pH]_{in}$ of a fraction of the conjugated K562 target cells changed. The direction of the change (acidification or alkalinization) depended in general on $[pH]_{ex}$, indicating that an equilibration with $[pH]_{ex}$ rather than an active cellular process was taking place. An additional decrease in $[pH]_{in}$ was observed in dying cells immediately before the cell died. This result, however, needs to be interpreted with caution since the low fluorescence signals, which were usually measured at that time, could lead to an underestimation of the ratio. The change in $[pH]_{in}$ was usually accompanied by an increased membrane permeability, i.e., leakage of BCECF out of the cell (Fig. 5, open symbols). Similar to the leakage of Fura-2, the cell membrane became either completely permeable to BCECF (dying cells) or partly (Fig. 5, transient cells: asterisks) during the 10 min observation time. In most cases where the dye completely leaked out of the cell, the leakage occurred in one step with a half-time of approximately 70 s. In cases of partial permeability, $[pH]_{in}$ did not return to the initial level but rather remained on the changed level for the time the cells were followed. Changes in $[pH]_{in}$ were observed neither in the non-conjugated K562 cells nor in the control K562 cells (incubated without NK cells).

Effect of $[pH]_{ex}$ on the Cytotoxic Process

The measurements of $[Ca^{2+}]_{in}$ and $[pH]_{in}$ were used to resolve whether $[pH]_{ex}$ affects the killing mechanism that leads to immediate cell death. The efficiency of the process and the average programming and killing times were determined. The programming time was defined as the time from adding calcium to the conjugates to the time that a change in the physiological parameter was detected. The killing time was defined as the time between detecting the first change to the moment of cell death (i.e., dye completely leaked out of the cell).

Figure 6 shows the effect of $[pH]_{ex}$ on the number of dead cells relative to the number of cells that underwent a change in the physiological parameter. At lower $[pH]_{ex}$ (6.8–7.0), almost all cells that underwent a change died within 10 min after the change was detected. At $[pH]_{ex}$ higher than 7.0, the average number of dead cells was approximately 70%. Figure 7 shows the effect of $[pH]_{ex}$ on the programming (hatched bars) and killing (black bars) times. The programming time seems to be sensitive to the $[pH]_{ex}$: it was shortest at $[pH]_{ex}$ 7.3–7.6 (approximately 3 min). The killing time was not significantly dependent on $[pH]_{ex}$ and was approximately 3 min.

DISCUSSION

Our results demonstrate two different types of target cell response to the attack by an NK cell. A target cell either dies immediately (on the average within 3 min; Fig. 7), due to a complete breakdown of the membrane impermeability ("dying cells"), or it manages to repair the initial damage and survives ("transient cells"). These two responses may correspond to two distinct killing mechanisms employed by NK cells (23). Another possible explanation is that individual target cells differ in their *sensitivity* to the NK cell attack or that individual NK cells differ in their *killing capacity* (due to higher concentration of the killing molecules?). The immediate cell death probably reflects the action of perforin, i.e., formation of pores in the target cell membrane which lead to osmotic imbalance and to the burst of the target cell. The *transiently* increased membrane permeability we observe is similar to the one previously observed upon treatment of the cells with sublethal doses of perforin (9), clearly indicating the repair capability of the cells (14).

The attack by an NK cell leads to an increase of $[Ca^{2+}]_{in}$ in both dying and transient cells (Fig. 4). An increase of $[Ca^{2+}]_{in}$ in the target cell during the attack of a cytotoxic cell has been described previously (1,13,

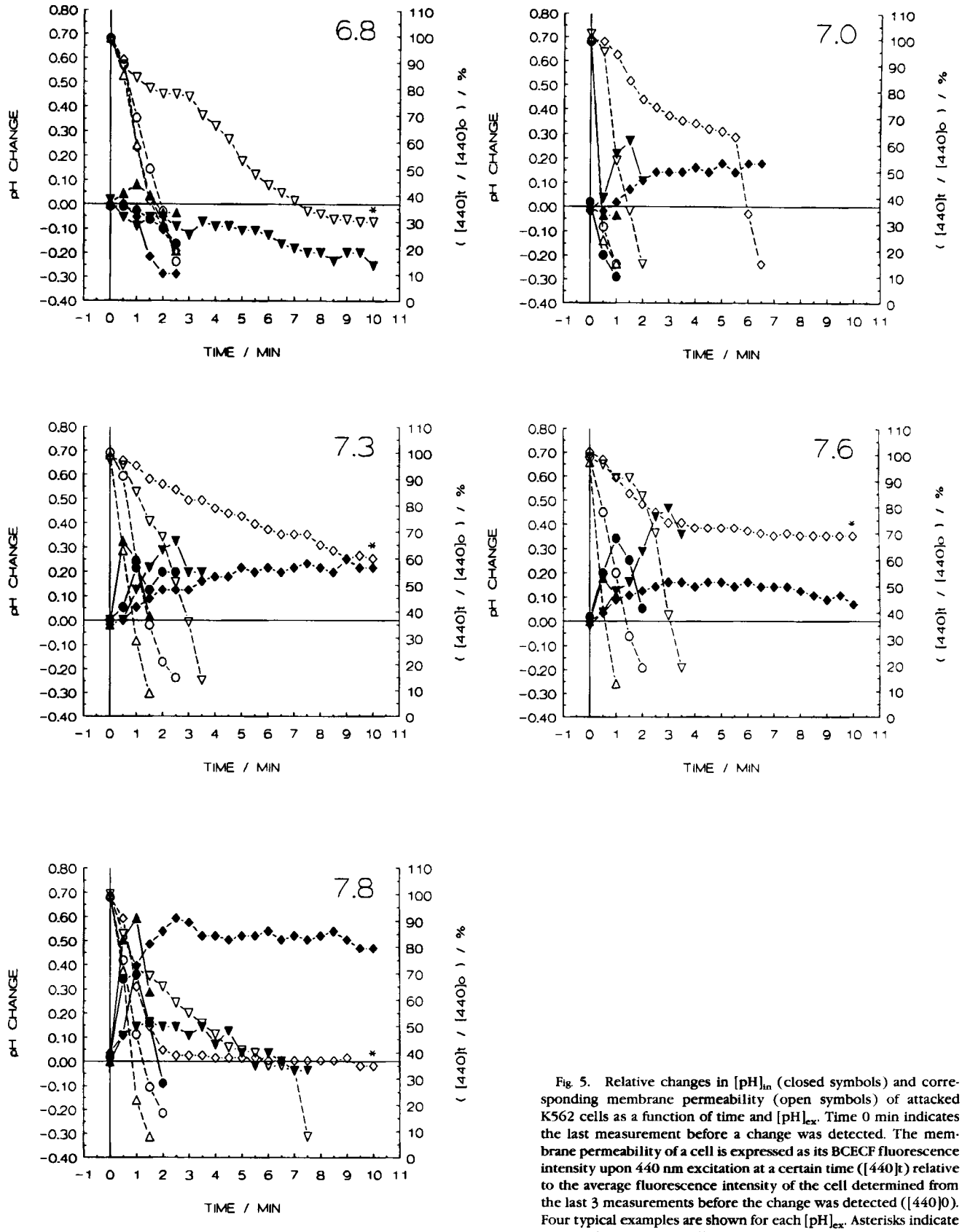

Fig. 5. Relative changes in $[pH]_{in}$ (closed symbols) and corresponding membrane permeability (open symbols) of attacked K562 cells as a function of time and $[pH]_{ex}$. Time 0 min indicates the last measurement before a change was detected. The membrane permeability of a cell is expressed as its BCECF fluorescence intensity upon 440 nm excitation at a certain time ([440]t) relative to the average fluorescence intensity of the cell determined from the last 3 measurements before the change was detected ([440]0). Four typical examples are shown for each $[pH]_{ex}$. Asterisks indicate transiently permeable cells.

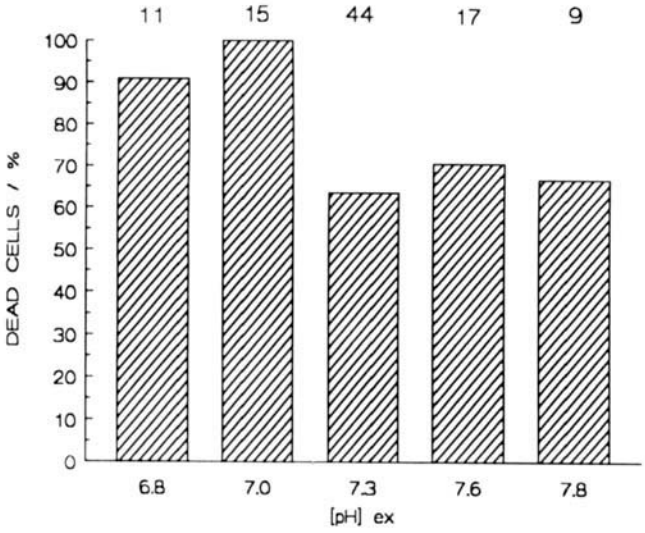

Fig. 6. Effect of $[pH]_{ex}$ on the immediate killing process. The number of dead K562 cells relative to the total number of cells that underwent a change in $[Ca^{2+}]_{in}$ or $[pH]_{in}$ was determined at different $[pH]_{ex}$. The total number of cells that underwent a change is indicated above the bars.

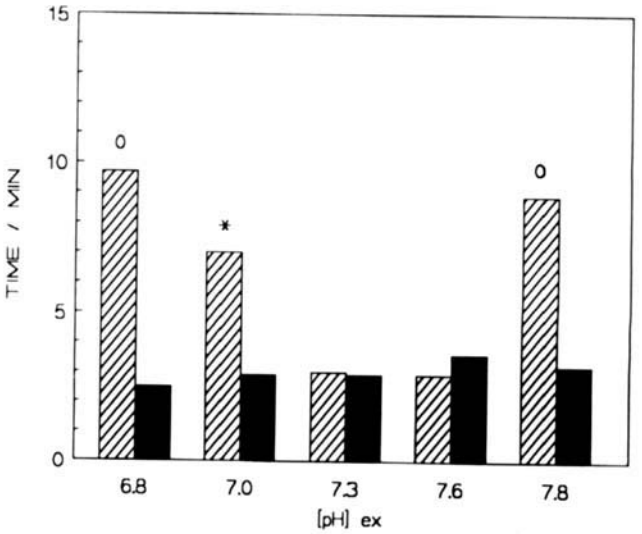

Fig. 7. Effect of $[pH]_{ex}$ on programming (hatched bars) and killing (black bars) times. The presented results are average values of 10 ($[pH]_{ex}$ 6.8), 15 ($[pH]_{ex}$ 7.0), 28 ($[pH]_{ex}$ 7.3), 12 ($[pH]_{ex}$ 7.6), and 6 ($[pH]_{ex}$ 7.8) cells. $^{*}P < 0.01$ and $^{o}P < 0.001$ (significantly different from the time at $[pH]_{ex}$ 7.3).

19,26,28), although the distinction between transient and dying cells has not been stated clearly. The average $[Ca^{2+}]_{in}$ level reached is higher in the dying cells (approximately 1,400 nM) than in the transient cells (approximately 700 nM).

The initial fast increase of $[Ca^{2+}]_{in}$ we observed is probably largely due to increased membrane permeability and passive influx of $[Ca^{2+}]_{in}$. However, transient cells were occasionally undergoing an additional increase of $[Ca^{2+}]_{in}$ without detectable loss of the dye, indicating that an active mechanism may also be involved in the increase of $[Ca^{2+}]_{in}$. An active influx of calcium may be due to depolarization of the target cell membrane (21), which could give rise to activation of voltage-dependent calcium channels (26).

In addition to an increase of $[Ca^{2+}]_{in}$, both dying and transient cells undergo changes in $[pH]_{in}$ (Fig. 5). These changes, however, primarily reflect an equilibration with $[pH]_{ex}$ due to the increased membrane permeability. Contrary to the changes of $[Ca^{2+}]_{in}$, $[pH]_{in}$ remained changed in transient cells during the observation time. This was observed even after the cell membrane became impermeable to the dye again. We are not sure whether the acidification, observed in the dying cells immediately before the cell died, is real or an artifact due to low fluorescence intensities that were usually measured at that time.

Our results show that upon the attack by an NK cell the target cell may die immediately, in a process resembling colloid osmosis, or it may repair the initial damage without an obvious immediate lethal effect. The *immediate* killing process is sensitive to $[pH]_{ex}$. It appears to be most efficient at $[pH]_{ex}$ 6.8–7.0, with the shortest programming time at $[pH]_{ex}$ 7.3–7.6 and a $[pH]_{ex}$ independent killing time (Figs. 6, 7).

In conclusion, we show that the K562 target cells undergo significant changes in the intracellular calcium and pH homeostases under the attack of cloned human NK cells. The existence of two different types of target cell response is clearly demonstrated.

ACKNOWLEDGMENTS

We thank Dr. R.L.H. Bolhuis (Den Hoed Cancer Center, Rotterdam) for providing the NK cell clone and I.M.J. Segers-Nolten and Y.M. Kraan for excellent technical assistance.

LITERATURE CITED

1. Allbritton NL, Verret CR, Wolley RC, Eisen HN: Calcium ion concentrations and DNA fragmentation in target cell destruction by murine cloned cytotoxic lymphocytes. J Exp Med 167:514–527, 1988.
2. Bright GR, Fisher GW, Rogowska J, Taylor DL: Fluorescence ratio imaging microscopy: Temporal and spatial measurements of cytoplasmic pH. J Cell Biol 104:1019–1033, 1987.
3. Campbell AK: Intracellular calcium: Friend or foe? Clin Sci 72:1–10, 1987.
4. Duke RC, Chervenak R, Cohen JJ: Endogenous endonuclease-induced DNA fragmentation: An early event in cell-mediated cytolysis. Proc Natl Acad Sci USA 80:6361–6365, 1983.
5. Duvall E, Wyllie AH: Death and the cell. Immunol Today 7:115–119, 1986.
6. Grynkiewicz G, Poenie M, Tsien RY: A new generation of Ca^{2+} indicators with greatly improved fluorescence properties. J Biol Chem 260:3440–3450, 1985.
7. Henkart PA: Mechanism of lymphocyte-mediated cytotoxicity. Annu Rev Immunol 4:31–58, 1985.
8. Hess SD, Oortgiesen M, Cahalan MD: Calcium oscillations in human T and natural killer cells depend upon membrane potential and calcium influx. J Immunol 150:2620–2633, 1993.
9. Jones J, Hallett MB, Morgan BP: Reversible cell damage by T-cell perforins. Calcium influx and propidium iodide uptake into K562 cells in the absence of lysis. Biochem J 267:303–307, 1990.
10. Kägi D, Ledermann B, Bürki K, Seiler P, Odermatt B, Olsen KJ, Po-

dack ER, Zinkernagel RM, Hengartner H: Cytotoxicity mediated by T cells and natural killer cells is greatly impaired in perforin-deficient mice. Nature 369:31–37, 1994.
11. Kolber MA, Quinones R, Gress RE, Henkart PA: Measurement of cytotoxicity by target cell release and retention of the fluorescent dye bis-carboxyethyl-carboxyfluorescein (BCECF). J Immunol Methods 108:255–264, 1988.
12. Martz E, Howell DM: CTL: Virus control cells first and cytolytic cells second? DNA fragmentation, apoptosis and the prelytic halt hypothesis. Immunol Today 10:79–86, 1989.
13. McConkey DJ, Chow SC, Orrenius S, Jondal M: NK cell-induced cytotoxicity is dependent on a Ca^{2+} increase in the target. FASEB J 4:2661–2664, 1990.
14. Morgan BP, Dankert JR, Esser AF: Recovery of human neutrophils from complement attack: Removal of the membrane attack complex by endocytosis and exocytosis. J Immunol 138:246–253, 1987.
15. Nakajima H, Henkart PA: Cytotoxic lymphocyte granzymes trigger a target cell internal disintegration pathway leading to cytolysis and DNA breakdown. J Immunol 152:1057–1063, 1994.
16. Nishioka WK, Welsh RM: Inhibition of cytotoxic T lymphocyte-induced target cell DNA fragmentation, but not lysis, by inhibitors of DNA topoisomerases I and II. J Exp Med 175:23–27, 1992.
17. Orrenius S, McCabe MJ, Nicotera P: Ca^{2+}-dependent mechanisms of cytotoxicity and programmed cell death. Toxicol Lett 64/65:357–364, 1992.
18. Ostergaard HL, Kane KP, Mescher MF, Clark WR: Cytotoxic T lymphocyte mediated lysis without release of serine esterase. Nature 330:71–74, 1987.
19. Poenie M, Tsien RY, Schmitt-Verhulst A-M: Sequential activation and lethal hit measured by $[Ca^{2+}]_i$ in individual cytolytic T cells and targets. EMBO J 6:2223–2232, 1987.
20. Radošević K, Garritsen HSP, van Graft M, de Grooth BG, Greve J: A simple and sensitive flow cytometric assay for the determination of the cytotoxic activity of human natural killer cells. J Immunol Methods 135:81–89, 1990.
21. Radošević K, Bakker Schut TC, van Graft M, de Grooth BG, Greve J: A flow cytometric study of the membrane potential of natural killer and K562 cells during the cytotoxic process. J Immunol Methods 161:119–128, 1993.
22. Russel JH: Internal disintegration model of cytotoxic lymphocyte-induced target cell damage. Immunol Rev 72:97–118, 1983.
23. Sevilla CL, Radcliff G, Mahle NH, Swartz S, Sevilla MD, Chores J, Callewaert DM: Multiple mechanisms of target cell disintegration are employed in cytotoxicity reactions mediated by human natural killer cells. Nat Immun Cell Growth Regul 8:20–36, 1989.
24. Shi L, Kraut RP, Aebersold R, Greenberg AH: A natural killer cell granule protein that induces DNA fragmentation and apoptosis. J Exp Med 175:553–566, 1992.
25. Tian Q, Streuli M, Saito H, Schlossman SF, Anderson P: A polyadenylate binding protein localized to the granules of cytolytic lymphocytes induces DNA fragmentation in target cells. Cell 67:629–639, 1991.
26. Tirosh R, Berke G: T-lymphocyte-mediated cytolysis as an excitatory process of the target. I. Evidence that the target cell may be the site of Ca^{2+} action. Cell Immunol 95:113–123, 1985.
27. Tschopp J, Nabholz M: Perforin-mediated target cell lysis by cytolytic T lymphocytes. Annu Rev Immunol 8:279–302, 1990.
28. Van Graft M, Kraan YM, Segers IMJ, Radošević K, de Grooth BG, Greve J: Flow cytometric measurement of $[Ca^{2+}]_i$ and pH_i in conjugated natural killer cells and K562 target cells during the cytotoxic process. Cytometry 14:257–264, 1993.
29. Young JD-E, Clark WR, Liu C-C, Cohn ZA: A calcium- and perforin-independent pathway of killing mediated by murine cytolytic lymphocytes. J Exp Med 166:1894–1899, 1987.
30. Young JD-E, Cohn ZA: Cellular and humoral mechanisms of cytotoxicity: Structural and functional analysis. Adv Immunol 41:269–332, 1987.
31. Zychlinsky A, Zheng LM, Liu C-C, Young JD-E: Cytolytic lymphocytes induce both apoptosis and necrosis in target cells. J Immunol 146: 393–400, 1991.